Rate-Splitting Multiple Access-based Cognitive Radio Network With ipSIC and CEEs

Xuesong Gao, Xingwang Li, *Senior Member, IEEE,* Congzheng Han, Ming Zeng, *Member, IEEE,* Hongwu Liu, *Senior Member, IEEE,* Shahid Mumtaz, *Senior Member, IEEE,* Arumugam Nallanathan, *Fellow, IEEE*

***Abstract*—In this paper, we study the outage and ergodic rate performance of a rate-splitting multiple access (RSMA)-based cognitive radio (CR) system, where the secondary transmitter aims to communicate with two RSMA users. Imperfect successive interference cancellation (ipSIC) and channel estimation errors (CEEs) are considered in the proposed analysis. Analytical expressions for the outage probability (OP) and the ergodic rate (ER) are calculated. For a deeper understanding, the asymptotic behavior of OP and ER at high signal-to-noise ratio (SNR) regimes are carried out. Illustrative simulation results are presented and reveal that: i) The OP decreases and the ER gradually increases with the increase of SNR, and eventually approaching a constant; ii) ipSIC and CEEs have a negative impact on the considered system; iii) The outage and ER performance of RSMA-based CR network outperforms CR-NOMA network due to its flexible control of interference; iv) The OP first decreases and then increases with the power allocated to the common message, and there exists an optimal power allocation factor to ensure the reliable performance.**

***Index Terms*—Cognitive radio, ergodic rate, imperfect successive interference cancellation (ipSIC), outage probability, rate-splitting multiple access.**

I. Introduction

Recently, the ever increasing demands for high data rates and the rapid development of intelligent terminals have led to the search for the higher efficient spectrum and massive connectivity schemes [1], [2]. As two promising candidate techniques of the future wireless communication networks, rate-splitting multiple access (RSMA) and cognitive radio (CR) have been widely studied since it have the capability to support massive connectivity and high spectral efficiency [3], [4].

Xuesong Gao and Xingwang Li are with the School of Physics and Electronic Information Engineering, Henan Polytechnic University, Jiaozuo, China (email: gaoxuesong@home.hpu.edu.cn, lixingwangbupt@gmail.com).

Congzheng Han is Middle Atmosphere and Global environment Observation (LAGEO) Institute of Atmospheric Physics, Chinese Academy of Sciences, Beijing, 100029, China (e-mail: c.han@mail.iap.ac.cn).

M. Zeng is with the Department of Electrical and Computer Engineering, Laval University, Quebec, QC G1V 0A6, Canada (e-mail: ming.zeng@gel.ulaval.ca).

Hongwu Liu is with the School of Information Science and Electrical Engineering, Shandong Jiaotong University, Jinan 250357, China (e-mail: liuhongwu@sdjtu.edu.cn).

Shahid Mumtaz is with the Instituto de Telecomunicacoes, Aveiro, Portugal (e-mail: smumtaz@av.it.pt).

Arumugam Nallanathan is with the School of Electronic Engineering and Computer Science, Queen Mary University of London, London E1 4NS, U.K. (e-mail: a.nallanathan@qmul.ac.uk).

RSMA has aroused a heated attention as a powerful multiple access technique [5]. The dominant feature of RSMA is that the message required by the each user is divided into a common part and a private part at the transmitter. The common parts of all users are combined into a common message for each user to decode, while the private parts are independently encoded as private message that can only be recovered by its own user [6], [7]. RSMA decodes partial interference and treats the rest as noise at the receiver [8]. Therefore, it enables flexible interference control and is considered as a bridge between non-orthogonal multiple access (NOMA) and space-division multiple access (SDMA) [9], [10].

On a parallel avenue, cognitive radio (CR) is known as a potential technique that can effectively improve spectrum utilization [11]. The CR network consists of a primary network and a secondary network. It provides an opportunity for the secondary network to share the licensed spectrum with the primary network. In general, underlay, overlay and interweave are the three typical modes in CR network according to the different spectrum access paradigms. Among these, underlay CR is more appealing since it needs less collaborative overhead and low implementation complexity [12]. In underlay network, the secondary network can access the spectrum of the primary network for communication as long as its interference power to the primary network is within a certain power constraint [13].

RSMA combines the advantages of NOMA and SDMA, achieving massive connection, flexibly interference control and data transmission, while avoiding the complex receiver design problem in NOMA. Furthermore, CR compensates for the shortcomings of static spectrum allocation by dynamically accessing idle spectrum through spectrum monitoring. Therefore, applying rate splitting (RS) strategy to CR network will further improve the system performance and alleviate the problem of spectrum efficiency. In [14], the authors proposed an underlay multiple-input single-output network based on the downlink RSMA, and achieved the goal of minimizing the total transmit power by optimizing the precode vectors and common rate variables. The authors in [15] introduced RSMA into the downlink multi-antenna multi-carrier CR network and maximized the ergodic mutual information of secondary users under the consideration of imperfect channel state information (CSI) at transmitter. However, the above literature did not take imperfect successive interference cancellation (ipSIC) into account and were all focused on optimization rather than performance analysis. Liu *et al.* in [16] introduced RS strategy into an uplink CR-NOMA system, and proved the superiority of the RS for considered system's reliability by analyzing the outage probability (OP) of users.

Currently, most works on the combination of CR and RSMA focus on optimizing network models to achieve better performance. Unfortunately, the works of performance analysis are quite few. In [16], Liu *et al.* proposed an uplink RS-based CR system with Rayleigh fading channels. There also exist many differences between uplink and downlink of the networks, and thus, the analysis for uplink may not be applied to downlink. To the best of our knowledge, the work on the RMSA-underlay CR network is not available yet. Although both amplify-and-forward (AF) and underlay CR can improve the performance of primary users, these are two different schemes. Underlay CR communicates in two networks, while AF protocol has the drawback of noise amplification in the process of signal amplification. Motivated by above, the underlay CR is adopted. In addition, there was no work to introduce Nakagami-m fading channels into RSMA-based underlay CR networks and the current studies do not consider the impact of ipSIC and the channel estimation errors (CEEs). To fill this gap, RS strategy is adopted in the downlink underlay CR network in this paper. Secondary transmitter communicates with the secondary receivers without affecting the quality of service (QoS) of the primary network. The main contributions of this paper are as follows: 1) We analyze the OP and ER of the RSMA-based CR networks based on Nakagami-m fading channels under CEEs and ipSIC; 2) We discuss in depth the asymptotic performance of OP and ER at high signal-to-noise ratio (SNR) regions to shed light into the considered network; 3) We validate the advantage of the proposed RSMA-based CR networks by comparing with CR-NOMA networks.

II. SYSTEM MODEL

We consider a downlink RSMA-based underlay CR system, which consists of one secondary transmitter ST, one far user SR_f, one near user SR_n and one primary user PR. The following assumptions are considered: i) All nodes are equipped with a single antenna; ii) All channels are subject to the independent non-identically Nakagami-m fading channels [1].

As [17], linear minimum mean square error (LMMSE) algorithm is adopted since the perfect CSI is impossible to acquire. Thus, the channel coefficient can be denoted by

$$h_i = \hat{h}_i + e_i, i \in \{SR_f, SR_n, SP\}, \tag{1}$$

where $\hat{h}_i$ represents the estimated channel coefficient and $e_i \sim \mathcal{CN}\left(0, \sigma_{e_i}^2\right)$ is the CEE. In addition, secondary communication is allowed if the PR does not receive harmful interference from the ST. Accordingly, the following restriction should be met at the ST: $P_s = \min\left(P_{\max}, \frac{P_I}{\left|\hat{h}_{SP}\right|^2}\right)$, where $P_{\max}$ is the maximum transmit power of ST, and P_I represents the interference of ST on PR.

[1]Nakagami-m fading channel is a general fading channel, and it can reduce to Gaussian fading channel, Rayleigh fading channel and Rician fading channel by setting $m_i = 1/2$, $m_i = 1$ and $m_i = \frac{(K+1)^2}{2K+1}$, respectively, where K is the Rician factor.

According to the RSMA protocol, the signal transmitted by the ST can be written as

$$x_s = \sqrt{\alpha_c P_s} x_c + \sum_{k=1}^{2} \sqrt{\alpha_{p,k} P_s} x_{p,k}, \tag{2}$$

where α_c and $\alpha_{p,1}$, $\alpha_{p,2}$ are the power allocation factors of common message and private messages of the SR_f and SR_n, respectively, satisfying $\alpha_c + \sum_{k=1}^{2} \alpha_{p,k} = 1$.

The received message at SR_i $(i = f, n)$ can be expressed as

$$y_{SR_i} = \left(\hat{h}_{SR_i} + e_{SR_i}\right) x_s + n_{SR_i}, \tag{3}$$

where $n_i \sim \mathcal{CN}(0, N_i)$ denotes the complex additive white Gaussian noise (AWGN).

The signal-interference-plus-noise ratio (SINR) of decoding the common message x_c and private message $x_{p,k}$ for SR_i is given by

$$\gamma_{SR_i}^{x_c} = \frac{\left|\hat{h}_{SR_i}\right|^2 \gamma_s \alpha_c}{\left|\hat{h}_{SR_i}\right|^2 \gamma_s \sum\limits_{k=1}^{2} \alpha_{p,k} + \sigma_{e_{SR_i}}^2 \gamma_s + 1}, \tag{4}$$

$$\gamma_{SR_i}^{x_{p,i}} = \frac{\left|\hat{h}_{SR_i}\right|^2 \gamma_s \alpha_{p,k}}{\zeta \left|\hat{h}_{SR_i}\right|^2 \gamma_s \alpha_c + \left|\hat{h}_{SR_i}\right|^2 \gamma_s \sum\limits_{i=1, i\neq k}^{2} \alpha_{p,i} + \sigma_{e_{SR_i}}^2 \gamma_s + 1}, \tag{5}$$

where $\gamma_s = \frac{P_s}{N_0}$, ζ is a coefficient that represents the level of ipSIC, and satisfies $0 \leq \zeta \leq 1$. $\zeta = 0$ and $\zeta = 1$ represent perfect SIC and no SIC, respectively.

III. PERFORMANCE ANALYSIS

This section evaluates the outage and ER performance of the RSMA-based underlay CR network by calculating the analytcal expressions for OP and ER. Furthermore, we analyze the asymptotic behavior of OP and ER at high SNR regimes for the users to have a comprehensive sight of the proposed system.

A. Outage Performance Analysis

1) Outage Probability of SR_i: When both the common message x_c and private message $x_{p,k}$ can be successfully decoded by SR_i, the outage behavior will not occur. Therefore, the OP of SR_i can be denoted as

$$P_{out}^{SR_i} = 1 - \left[\Pr\left(\gamma_{SR_i}^{x_c} > \gamma_{th}^{c}, \gamma_{SR_i}^{p,i} > \gamma_{th}^{p,i}, P_{\max} \leq \frac{P_I}{\left|\hat{h}_{SP}\right|^2}\right) + \Pr\left(\gamma_{SR_i}^{x_c} > \gamma_{th}^{c}, \gamma_{SR_i}^{p,i} > \gamma_{th}^{p,i}, P_{\max} > \frac{P_I}{\left|\hat{h}_{SP}\right|^2}\right)\right], \tag{6}$$

where γ_{th}^{c} and $\gamma_{th}^{p,i}$ are the target rate of decoding x_c and $x_{p,k}$ of SR_i.

Theorem 1: For Nakagami-m fading channels, the OP of SR_f is represented as

$$P_{out}^{SR_f} = 1 - \left[e^{-A_1} \sum_{g_1=0}^{m_{SR_f}-1} \frac{{A_1}^{g_1}}{g_1!} \left(1 - e^{-A_2} \sum_{g_3=0}^{m_{SP}-1} \frac{{A_2}^{g_3}}{g_3!} \right) \right.$$
$$+ e^{-A_3 \sigma_{e_{SR_f}}^2 P_I} \left(\frac{m_{SP}}{\Omega_{SP}} \right)^{m_{SP}} \frac{1}{\Gamma(m_{SP})} \sum_{g_1=0}^{m_{SR_f}-1} \sum_{k_1=0}^{g_1} \frac{{A_3}^{g_1}}{g_1!}$$
$$\left. \times \binom{g_1}{k_1} \left(\sigma_{e_{SR_f}}^2 P_I \right)^{g_1-k_1} {A_4}^{-k_1-m_{SP}} A_5 \right], \tag{7}$$

where the integer m_i represents the fading severity parameter, Ω_i denotes the average power and its value is positive, $\Delta_1 = \frac{\gamma_{th}^c}{\alpha_c \gamma_s - \gamma_{th}^c \gamma_s \sum_{k=1}^2 \alpha_{p,k}}$, $\Delta_2 = \frac{\gamma_{th}^{p,f}}{\alpha_{p,1}\gamma_s - \zeta \alpha_c \gamma_s \gamma_{th}^{p,f} - \gamma_{th}^{p,f} \gamma_s \alpha_{p,2}}$, $\Delta_3 = \max(\Delta_1, \Delta_2)$, $\Delta_4 = \max\left(\frac{\gamma_{th}^c}{\alpha_c P_I - \gamma_{th}^c P_I \sum_{k=1}^2 \alpha_{p,k}}, \frac{\gamma_{th}^{p,f}}{\alpha_{p,1} P_I - \zeta \alpha_c P_I \gamma_{th}^{p,f} - \gamma_{th}^{p,f} P_I \alpha_{p,2}} \right)$, $A_1 = \frac{m_{SR_f} \Delta_3 \left(\sigma_{e_{SR_f}}^2 \gamma_s + 1 \right)}{\Omega_{SR_f}}$, $A_2 = \frac{m_{SP} P_I}{\Omega_{SP} P_{\max}}$, $A_3 = \frac{m_{SR_f} \Delta_4}{\Omega_{SR_f}}$, $A_4 = \frac{m_{SR_f} \Delta_4 \Omega_{SP} + m_{SP} \Omega_{SR_f}}{\Omega_{SR_f} \Omega_{SP}}$, $A_5 = \Gamma\left(k_1 + m_{SP}, \frac{P_I A_4}{P_{\max}} \right)$, and $\gamma_s = \frac{P_{\max}}{N_1}$.

Proof: See Appendix A.

Corollary 1: At high SNRs, the asymptotic expression of OP for SR_f is given by

$$P_{out,\gamma\to\infty}^{SR_f} = 1 - e^{-A_1} \sum_{g_1=0}^{m_{SR_f}-1} \frac{{A_1}^{g_1}}{g_1!}. \tag{8}$$

Next, the optimal value of α_c are derived to achieve the optimal reliability of the SR_f by performing a series of calculations on Eq. (8). We set $\alpha_{p,1} = b_1(1-\alpha_c)$ and $\alpha_{p,2} = b_2(1-\alpha_c)$, where $b_1 > b_2$ and $b_1 + b_2 = 1$. $\Delta_1 = \frac{\gamma_{th}^c}{\alpha_c A - B}$ and $\Delta_2 = \frac{\gamma_{th}^{p,f}}{\alpha_c C + D}$, where $A = \gamma_s + \gamma_{th}^c \gamma_s$, $B = \gamma_{th}^c \gamma_s$, $C = b_2 \gamma_{th}^{p,f} \gamma_s - b_1 \gamma_s - \zeta \gamma_s \gamma_{th}^{p,f}$ and $D = b_1 \gamma_s - b_2 \gamma_s \gamma_{th}^{p,f}$. It is obvious that $A > 0$ and $C < 0$, so the values of Δ_1 and Δ_2 decrease and increase with respect to a_c, respectively. Accordingly, $P_{out,\gamma\to\infty}^{SR_f}$ will reach its optimal value when Δ_1=Δ_2. Therefore, the optimal power allocation coefficient for the common messages $\alpha_c = \frac{D\gamma_{th}^c + B\gamma_{th}^{p,f}}{A\gamma_{th}^{p,f} - C\gamma_{th}^c}$. Similarly, the optimal value for the SR_n can be computed using the similar methodology.

Similarly, the following *Theorem* gives the analytical OP expression of SR_n.

Theorem 2: For Nakagami-m fading channels, the analytical expression for the OP of SR_n is represented as

$$P_{out}^{SR_n} = 1 - \left[e^{-A_6} \sum_{g_2=0}^{m_{SR_n}-1} \frac{{A_6}^{g_2}}{g_2!} \left(1 - e^{-A_2} \sum_{g_3=0}^{m_{SP}-1} \frac{{A_2}^{g_3}}{g_3!} \right) \right.$$
$$+ e^{-A_7 \sigma_{e_{SR_n}}^2 P_I} \left(\frac{m_{SP}}{\Omega_{SP}} \right)^{m_{SP}} \frac{1}{\Gamma(m_{SP})} \sum_{g_2=0}^{m_{SR_n}-1} \sum_{k_2=0}^{g_2} \frac{{A_7}^{g_2}}{g_2!}$$
$$\left. \times \binom{g_2}{k_2} \left(\sigma_{e_{SR_n}}^2 P_I \right)^{g_2-k_2} {A_8}^{-k_2-m_{SP}} A_9 \right], \tag{9}$$

where $A_6 = \frac{m_{SR_f} \Delta_5 \left(\sigma_{e_{SR_f}}^2 \gamma_s + 1 \right)}{\Omega_{SR_f}}$, $A_7 = \frac{m_{SR_n} \Delta_6}{\Omega_{SR_n}}$, $A_8 = \frac{m_{SR_n} \Delta_6 \Omega_{SP} + m_{SP} \Omega_{SR_n}}{\Omega_{SR_n} \Omega_{SP}}$, $A_9 = \frac{m_{SR_n} \Delta_6 \Omega_{SP} + m_{SP} \Omega_{SR_n}}{\Omega_{SR_n} \Omega_{SP}}$, $A_{10} = \Gamma\left(k_2 + m_{SP}, \frac{P_I A_8}{P_{\max}} \right)$, $\Delta_5 = \max\left(\frac{\gamma_{th}^c}{\alpha_c \gamma_s - \gamma_{th}^c \gamma_s \sum_{k=1}^2 \alpha_{p,k}}, \frac{\gamma_{th}^{p,n}}{\alpha_{p,2}\gamma_s - \zeta \alpha_c \gamma_s \gamma_{th}^{p,n} - \gamma_{th}^{p,n} \gamma_s \alpha_{p,1}} \right)$, and $\Delta_6 = \max\left(\frac{\gamma_{th}^c}{\alpha_c P_I - \gamma_{thc} P_I \sum_{k=1}^2 \alpha_{p,k}}, \frac{\gamma_{th}^{p,n}}{\alpha_{p,2} P_I - \zeta \alpha_c P_I \gamma_{th}^{p,n} - \gamma_{th}^{p,n} P_I \alpha_{p,1}} \right)$.

Corollary 2: The asymptotic OP expression for SR_n at high SNRs can be written as

$$P_{out,\gamma\to\infty}^{SR_n} = 1 - e^{-A_6} \sum_{g_2=0}^{m_{SR_n}-1} \frac{{A_6}^{g_2}}{g_2!}. \tag{10}$$

For a deeper exploration of the RSMA-based underlay CR network, we analyze the diversity orders of SR_f and SR_n. The diversity order is represented as

$$d = -\lim_{\gamma\to\infty} \frac{\log\left(P_{out}^{\infty}\right)}{\log\gamma}. \tag{11}$$

Corollary 3: The diversity orders of SR_f, SR_n can be represented as

$$d_{SR_f} = d_{SR_n} = 0. \tag{12}$$

Remark 1: From *Corollaries 1* and *2*, we can observe that the OP of SR_f and SR_n decreases with P_I, the reliability continues to increase, and eventually saturates to a constant. This implies that the OPs have error floors, resulting in the diversity orders to be 0. In addition, there is an optimal value for α_c to ensure the most reliable performance for the considered system.

B. Ergodic Rate Analysis

The analytical expression for the ER of SR_i can be represented as

$$R_{SR_i} = \begin{cases} E\left[\log_2\left(1+\gamma_{SR_i}^{x_c}\right)\right] + E\left[\log_2\left(1+\gamma_{SR_i}^{x_{p,i}}\right)\right] \\ \quad (P_s = P_{\max}) \\ E\left[\log_2\left(1+\gamma_{SR_i}^{x_c}\right)\right] + E\left[\log_2\left(1+\gamma_{SR_i}^{x_{p,i}}\right)\right] \\ \quad (P_s = P_I) \end{cases}. \tag{13}$$

Unfortunately, it is very difficult, if not impossible, to obtain exact expressions for the ERs of SR_f and SR_n. To this end, we seek to obtain the approximations of the ER of the two users in the following *Theorem*.

Theorem 3: For Nakagami-m fading channels, the analytic expression for the ER of SR_f is approximately denoted by

$$R_{SR_f} \approx \log_2(1+\phi_1) + \log_2(1+\phi_2)$$
$$+ \log_2(1+\phi_3) + \log_2(1+\phi_4), \tag{14}$$

where $\phi_1 = \Omega_{SR_f}\gamma_s\alpha_c \Big/ \left(\Omega_{SR_f}\gamma_s \sum_{k=1}^2 \alpha_{p,k} + \sigma_{e_{SR_f}}^2 \gamma_s + 1 \right)$, $\phi_2 = \Omega_{SR_f}\gamma_s\alpha_{p,1} \Big/ \left(\zeta\Omega_{SR_f}\alpha_c\gamma_s + \Omega_{SR_f}\gamma_s\alpha_{p,2} + \sigma_{e_{SR_f}}^2 \gamma_s + 1 \right)$, $\phi_3 = \Omega_{SR_f} P_I \alpha_c \Big/ \left(\Omega_{SR_f} P_I \sum_{k=1}^2 \alpha_{p,k} + \sigma_{e_{SR_f}}^2 P_I + A_{11} \right)$, and $\phi_4 = \Omega_{SR_f} P_I \alpha_{p,1} \Big/ \left(\zeta\Omega_{SR_f}\alpha_c P_I + \Omega_{SR_f} P_I \alpha_{p,2} + A_{11} \right)$, and $A_{11} = \frac{\Omega_{SP}\Gamma(m_{SP}+1, m_{SP}P_I/\Omega_{SP}P_{\max})}{m_{SP}\Gamma(m_{SP})}$.

Proof: See Appendix B.

Corollary 4: At high SNRs, the asymptotic expression for ER of SR_f can be written as

$$\begin{aligned} R_{SR_f}^{\infty} &= \log_2\left(1+{\phi_1}'\right)+\log_2\left(1+{\phi_2}'\right) \\ &\quad +\log_2\left(1+\phi_3\right)+\log_2\left(1+\phi_4\right), \end{aligned} \tag{15}$$

where ${\phi_1}' = \Omega_{SR_f}\alpha_c \Big/ \left(\Omega_{SR_f}\sum_{k=1}^{2}\alpha_{p,k}+\sigma_{e_{SR_f}}^2\right)$ and $\phi_2' = \Omega_{SR_f}\alpha_{p,1} \Big/ \left(\zeta\Omega_{SR_f}\alpha_c+\Omega_{SR_f}\alpha_{p,2}+\sigma_{e_{SR_f}}^2\right)$.

Similar to SR_f, the following *Theorem* gives the ER of SR_n.

Theorem 4: For Nakagami-m fading channels, the analytical expression for the ER of SR_n is approximately written by

$$\begin{aligned} R_{SR_n} &\approx \log_2\left(1+\phi_5\right)+\log_2\left(1+\phi_6\right) \\ &\quad +\log_2\left(1+\phi_7\right)+\log_2\left(1+\phi_8\right), \end{aligned} \tag{16}$$

where $\phi_5 = \Omega_{SR_n}\gamma_s\alpha_c \Big/ \left(\Omega_{SR_n}\gamma_s\sum_{k=1}^{2}\alpha_{p,k} + \sigma_{e_{SR_n}}^2\gamma_s+1\right)$, $\phi_6 = \Omega_{SR_n}\gamma_s\alpha_{p,2}/(\zeta\Omega_{SR_n}\alpha_c\gamma_s + \Omega_{SR_n}\gamma_s\alpha_{p,1}+\sigma_{e_{SR_n}}^2\gamma_s+1\Big)$, $\phi_7 = \Omega_{SR_n}P_I\alpha_c/(\Omega_{SR_n}P_I\sum_{k=1}^{2}\alpha_{p,k}+\sigma_{e_{SR_n}}^2\gamma_s+A_{11})$ and $\phi_8 = \Omega_{SR_n}P_I\alpha_{p,2}/(\zeta\Omega_{SR_n}\alpha_cP_I+\Omega_{SR_n}P_I\alpha_{p,1}+\sigma_{e_{SR_n}}^2P_I + A_{11})$.

Corollary 5: At high SNRs, we obtain the ER asymptotic expression of SR_n as

$$\begin{aligned} R_{SR_n}^{\infty} &= \log_2\left(1+{\phi_5}'\right)+\log_2\left(1+{\phi_6}'\right) \\ &\quad +\log_2\left(1+\phi_7\right)+\log_2\left(1+\phi_8\right), \end{aligned} \tag{17}$$

where ${\phi_5}' = \Omega_{SR_n}\alpha_c \Big/ \left(\Omega_{SR_n}\sum_{k=1}^{2}\alpha_{p,k}+\sigma_{e_{SR_n}}^2\right)$ and ${\phi_6}' = \Omega_{SR_n}\alpha_{p,2} \Big/ \left(\zeta\Omega_{SR_n}\alpha_c+\Omega_{SR_n}\alpha_{p,1}+\sigma_{e_{SR_n}}^2\right)$.

Remark 2: From *Corollaries 4* and *5*, it can be observed that the ER increases with P_I and finally tends to be a fix constant, indicating that there exists a ceiling for ER. The ER of SR_f and SR_n increases with α_c, but decreases with the coefficients of ipSIC and CEEs. Therefore, a higher value of α_c is preferred and more accurate hardware devices should be selected to reduce the coefficients of ipSIC and CEEs.

IV. NUMERICAL RESULTS

The analysis of this work are corroborated by the Monte Carlo simulations. All experiments are established on 10^6 times. Unless stated explicitly, we have the following settings: The noise power are $N_0 = N_1 = 1$, The maximum transmit power of ST is $P_{\max} = 1$; The target rates are $\gamma_{th}^{c} = \gamma_{th}^{p,f} = \gamma_{th}^{p,n} = 0.1$; The power allocation coefficients for common and private message are $\alpha_c = 0.6$, $\alpha_{p,1} = 0.25$ and $\alpha_{p,2} = 0.15$; The fading severity parameters are $m_{SP} = 6$, $m_{SR_f} = 4$; $m_{SR_n} = 2$; The average power are $\Omega_{SP} = 4$, $\Omega_{SR_f} = 3$, $\Omega_{SR_n} = 4$; The channel estimation errors are $\sigma_{e_{SR_f}}^2 = \sigma_{e_{SR_n}}^2 = 0.08$; The ipSIC is $\zeta = 0.01$.

Fig. 1 presents the OP of the far user and near user versus P_I, respectively. We can clearly observe that OP decreases with P_I, while the reliability of the system increases with P_I, which can be deduced from (7) and (9). OP gradually reaches a fixed constant when P_I tends to infinity, resulting in an error floor. This is due to the flexible decoding method of RSMA. As the OP reaches saturation, the ability to increase the reliable performance of the system by adding P_I is no longer significant. In addition, it also find that the reliable of CR-RSMA system outperforms CR-NOMA system because of the flexible management of interference.

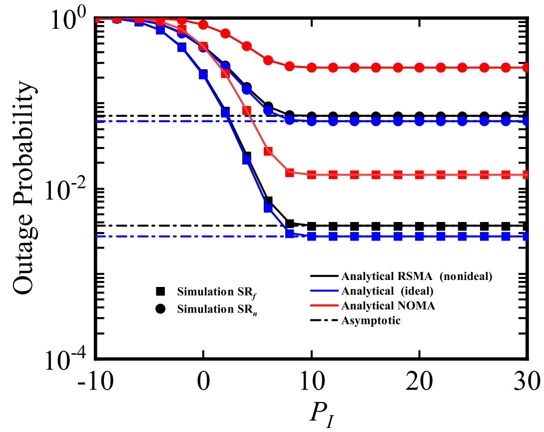

Fig. 1. The OP versus the P_I for ideal and non-ideal conditions

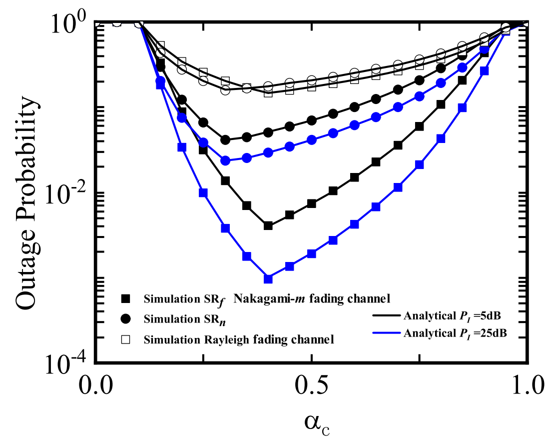

Fig. 2. The OP of users versus the α_c

Fig. 2 plots the effect of power allocation coefficient α_c on the reliable performance under the Nakagami-m fading channels and Rayleigh fading channels. It is clear that OP first decreases and then increases with α_c, showing a critical point. There exits an optimal α_c to minimize the OPs, and the system performance will deteriorate if α_c deviates from the optimal value. The larger α_c becomes, the larger corresponding power of common message and the smaller corresponding power of private message. The common message link is basically in an outage state if α_c is extremely small, vice versa. The change in the value of α_c causes the OP to generate the state shown in the Fig. 2. Furthermore, we consider the effect of different P_I values on user OP. It is not difficult to see that when the P_I gets larger, the performance improves better. In addition, we can observed that the OPs of SR_f and SR_n are smaller and the reliability is higher under the Nakagami-m fading channels.

Under ideal and nonideal conditions, the curves of ER are

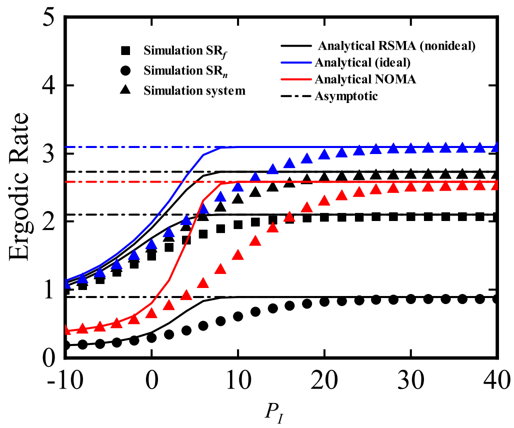

Fig. 3. The ER of users versus the P_I

depicted versus P_I in Fig. 3. The experiments are established on 10^5 times. We set $m_{SP} = 2$, $m_{SR_f} = 8$, $m_{SR_n} = 7$ $\Omega_{SP} = 2$, $\Omega_{SR_f} = 3$ and $\Omega_{SR_n} = 0.3$. It can be clearly seen that with the increase of P_I, the ER performance of the RSMA-based underlay CR system improves, which can be inferred from (14) and (16). The ER tends to be a fixed constant when P_I reaches infinity. As can be seen from the Fig. 3, the CEEs and ipSIC negatively affect the ER performance of the considered system. By comparing RSMA-based CR network with CR-NOMA, we find that RSMA system outperforms NOMA system for ER.

V. CONCLUSION

In this paper, we analyzed the outage and ER performance of the proposed RSMA-based CR systems. To obtain a better view of the system performance, the approximate behavior of OP and ER at high SNR were investigated. The simulation results showed that the OP decreases and the ER increases gradually with the transmit SNR of ST, and tended to be a fixed constant. Moreover, ipSIC and non-ideal CSI had a negative impact on the considered network. Finally, we found that the performance of RSMA-based CR networks was better than that of CR-NOMA networks.

APPENDIX A

Plugging (4) and (5) into (6), the OP of SR_f is given by

$$P_{out}^{SR_f} = 1 - \Bigg[\underbrace{\Pr\left(\gamma_{SR_f}^{x_c} > \gamma_{th}^{c}, \gamma_{SR_f}^{x_{p,f}} > \gamma_{th}^{p,f}, P_{\max} \le \frac{P_I}{\left|\hat{h}_{SP}\right|^2}\right)}_{I_1} + \underbrace{\Pr\left(\gamma_{SR_f}^{x_c} > \gamma_{th}^{c}, \gamma_{SR_f}^{x_{p,f}} > \gamma_{th}^{p,f}, P_{\max} > \frac{P_I}{\left|\hat{h}_{SP}\right|^2}\right)}_{I_2} \Bigg], \tag{A.1}$$

I_1 and I_2 can be denoted as

$$\begin{aligned} I_1 &= \int_{\Delta_3\left(\sigma_{e_{SR_f}}^2+1\right)}^{\infty} f_{|\hat{h}_{SR_f}|^2}(x)dx \int_0^{\frac{P_I}{P_{\max}}} f_{|\hat{h}_{SP}|^2}(y)dy \\ &= e^{-A_1} \sum_{g_1=0}^{m_{SR_f}-1} \frac{{A_1}^{g_1}}{g_1!} \left(1 - e^{-A_2} \sum_{g_3=0}^{m_{SP}-1} \frac{{A_2}^{g_3}}{g_3!}\right), \end{aligned} \tag{A.2}$$

$$\begin{aligned} I_2 &= \int_{\frac{P_I}{P_{\max}}}^{\infty} \int_{\Delta_4\left(\sigma_{e_{SR_f}}^2 P_I + y\right)}^{\infty} f_{|\hat{h}_{SR_f}|^2}(x) f_{|\hat{h}_{SP}|^2}(y) dx dy \\ &= e^{-A_3 \sigma_{e_{SR_f}}^2 P_I} \left(\frac{m_{SP}}{\Omega_{SP}}\right)^{m_{SP}} \frac{1}{\Gamma\left(m_{SP}\right)} \sum_{g_1=0}^{m_{SR_f}-1} \sum_{k_1=0}^{g_1} \frac{{A_3}^{g_1}}{g_1!} \\ &\times \binom{g_1}{k_1} \left(\sigma_{e_{SR_f}}^2 P_I\right)^{g_1-k_1} {A_4}^{-k_1-m_{SP}} A_5, \end{aligned} \tag{A.3}$$

In conclusion, (A.2) and (A.3) are substituted into (A.1) to obtain (7).

The solution process of outage performance for SR_n is similar to SR_f, so it is omitted due the space limited.

APPENDIX B

Substituting (4) and (5) into (13), the ER of SR_f can be expressed as

$$\begin{aligned} R_{SR_f} \approx{}& \log_2\left[1 + E\left(\phi_9\right)\right] + \log_2\left[1 + E\left(\phi_{10}\right)\right] \\ &+ \log_2\left[1 + E\left(\phi_{11}\right)\right] + \log_2\left[1 + E\left(\phi_{12}\right)\right]. \end{aligned} \tag{B.1}$$

where $\phi_9 = \frac{E\left(\left|\hat{h}_{SR_f}\right|^2\right)\gamma_s\alpha_c}{E\left(\left|\hat{h}_{SR_f}\right|^2\right)\gamma_s \sum_{k=1}^{2} \alpha_{p,k} + \sigma_{e_{SR_f}}^2 \gamma_s + 1}$, $\phi_{10} = \frac{E\left(\left|\hat{h}_{SR_f}\right|^2\right)\gamma_s\alpha_{p,1}}{\zeta E\left(\left|\hat{h}_{SR_f}\right|^2\right)\alpha_c\gamma_s + E\left(\left|\hat{h}_{SR_f}\right|^2\right)\gamma_s\alpha_{p,2} + \sigma_{e_{SR_f}}^2 \gamma_s + 1}$, $\phi_{11} = \frac{E\left(\left|\hat{h}_{SR_n}\right|^2\right)P_I\alpha_c}{E\left(\left|\hat{h}_{SR_n}\right|^2\right)P_I \sum_{k=1}^{2} \alpha_{p,k} + \sigma_{e_{SR_n}}^2 P_I + E\left(\left|\hat{h}_{SP}\right|^2\right)}$ and $\phi_{12} = \frac{E\left(\left|\hat{h}_{SR_n}\right|^2\right)P_I\alpha_{p,1}}{\zeta E\left(\left|\hat{h}_{SR_n}\right|^2\right)\alpha_c P_I + E\left(\left|\hat{h}_{SR_n}\right|^2\right)P_I\alpha_{p,2} + \sigma_{e_{SR_f}}^2 P_I + E\left(\left|\hat{h}_{SP}\right|^2\right)}$. where $E\left(\left|\hat{h}_{SR_f}\right|^2\right) = \int_0^{+\infty} x f_{\left|\hat{h}_{SR_f}\right|^2}(x)\, dx = \Omega_{SR_f}$.

Similarly, we can get $E\left(\left|\hat{h}_{SR_n}\right|^2\right) = \Omega_{SR_n}$ and $E\left(\left|\hat{h}_{SP}\right|^2\right) = \frac{\Omega_{SP}\Gamma(m_{SP}+1, m_{SP}P_I/\Omega_{SP}P_{\max})}{m_{SP}\Gamma(m_{SP})}$.

The ER for SR_n is similar to SR_f, so it also be omitted due the space limited.

REFERENCES

[1] S. Khisa, M. Almekhlafi, M. Elhattab, and C. Assi, “Full duplex cooperative rate splitting multiple access for a MISO broadcast channel with two users,” *IEEE Commun. Lett.*, vol. 26, no. 8, pp. 1913-1917, Aug. 2022.

[2] X. Li, Q. Wang, M. Zeng, Y. Liu, S. Dang, T. A. Tsiftsis and O. A. Dobre, “Physical-Layer Authentication for Ambient Backscatter Aided NOMA Symbiotic Systems,” *IEEE Trans. Commun.*, vol. 71, no. 4, pp. 2288-2303, Apr. 2023.

[3] J. Huang, Y. Yang, L. Yin, D. He, and Q. Yan, “Deep reinforcement learning-based power allocation for rate-splitting multiple access in 6G LEO satellite communication system,” *IEEE Wireless Commun. Lett.*, vol. 11, no. 10, pp. 2185-2189, Oct. 2022.

[4] A. Papadopoulos, N. D. Chatzidiamantis, and L. Georgiadis, "Network coding techniques for primary-secondary user cooperation in cognitive radio networks," *IEEE Trans. Wireless Commun*., vol. 19, no. 6, pp. 4195-4208, Jun. 2020.

[5] M. Katwe, K. Singh, B. Clerckx, and C. -P. Li, "Rate splitting multiple access for sum-rate maximization in IRS aided uplink communications," *IEEE Trans. Wireless Commun*., 2022, doi: 10.1109/TWC.2022.3210338.

[6] Y. Mao, E. Piovano, and B. Clerckx, "Rate-splitting multiple access for overloaded cellular Internet of Things," *IEEE Trans. Commun*., vol. 69, no. 7, pp. 4504-4519, Jul. 2021.

[7] W. Wang, L. Li, G. Deng, and J. Li, "A joint multi-service transmission scheme for RSMA-aided cell-free mMIMO system," *IEEE Commun. Lett*., doi: 10.1109/LCOMM.2022.3174111.

[8] L. Yin and B. Clerckx, "Rate-splitting multiple access for satellite-terrestrial integrated networks: Benefits of coordination and cooperation," *IEEE Trans. Wireless Commun*., 2022, doi: 10.1109/TWC.2022.3192980.

[9] H. Li, Y. Mao, O. Dizdar, and B. Clerckx, "Rate-splitting multiple access for 6G-Part III: Interplay with reconfigurable intelligent surfaces," *IEEE Commun. Lett*., vol. 26, no. 10, pp. 2242-2246, Oct. 2022.

[10] S. Park, J. Choi, J. Park, W. Shin and B. Clerckx, "Rate-Splitting Multiple Access for Quantized Multiuser MIMO Communications," *IEEE Trans. Wireless Commun*.

[11] X. Li et al., "Cognitive AmBC-NOMA IoV-MTS networks with IQI: Reliability and security analysis," *IEEE Trans. Intell. Transp. Syst*., early access, Sep. 27, 2021, doi: 10.1109/TITS.2021.3113995.

[12] X. Li et al., "Physical layer security of cognitive ambient backscatter communications for green Internet-of-Things," *IEEE Trans. Green Commun. Netw*., vol. 5, no. 3, pp. 1066-1076, Sep. 2021.

[13] W. Lee and K. Lee, "Deep learning-aided distributed transmit power control for underlay cognitive radio Network," *IEEE Trans. Veh. Technol*., vol. 70, no. 4, pp. 3990-3994, Apr. 2021.

[14] M. R. Camana, C. E. Garcia, and I. Koo, "Deep learning-assisted power minimization in underlay MISO-SWIPT systems based on rate-splitting multiple access," *IEEE Access*., vol. 10, pp. 62137-62156, Jun. 2022.

[15] O. Dizdar and B. Clerckx, "Rate-splitting multiple access for communications and jamming in multi-nntenna multi-carrier cognitive radio systems," *IEEE Trans. Inf. Forensics Security*., vol. 17, pp. 628-643, Feb. 2022.

[16] H. Liu, Z. Bai, H. Lei, G. Pan, K. J. Kim, and T. A. Tsiftsis, "A new rate splitting strategy for uplink CR-NOMA systems," *IEEE Trans. Veh. Technol*., vol. 71, no. 7, pp. 7947-7951, Apr. 2022.

[17] X. Li, J. Li, Y. Liu, Z. Ding, and A. Nallanathan, "Residual transceiver hardware impairments on cooperative NOMA networks," *IEEE Trans. Wireless Commun*., vol. 19, no. 1, pp. 680-695, Jan. 2020.